

## Electronic properties of the metallic pyrochlore ruthenates $\text{Pb}_2\text{Ru}_2\text{O}_{6.5}$ and $\text{Bi}_2\text{Ru}_2\text{O}_7$

Makoto Tachibana,<sup>1,2</sup> Yoshimitsu Kohama,<sup>2</sup> Tomotaka Shimoyama,<sup>2</sup> Akihiro Harada,<sup>2</sup> Tomoyasu Taniyama,<sup>2</sup> Mitsuru Itoh,<sup>2</sup> Hitoshi Kawaji,<sup>2</sup> and Tooru Atake<sup>2</sup>

<sup>1</sup>International Center for Young Scientists, National Institute for Materials Science, Namiki 1-1, Tsukuba, Ibaraki 305-0044, Japan

<sup>2</sup>Materials and Structures Laboratory, Tokyo Institute of Technology, 4259 Nagatsuta-cho, Midori-ku, Yokohama 226-8503, Japan

(Received 2 February 2006; published 22 May 2006)

We report the temperature dependence of the resistivity, magnetic susceptibility, and heat capacity of single crystalline  $\text{Pb}_2\text{Ru}_2\text{O}_{6.5}$  and  $\text{Bi}_2\text{Ru}_2\text{O}_7$ , the metallic members of the pyrochlore ruthenates. The analysis of the  $T^2$  coefficient of the resistivity, Pauli paramagnetic susceptibility, and linear heat-capacity coefficient indicates that  $\text{Pb}_2\text{Ru}_2\text{O}_{6.5}$  is a well-defined Fermi liquid with strong electron correlation. For  $\text{Bi}_2\text{Ru}_2\text{O}_7$ , thermodynamic data suggest moderately correlated behavior, while the resistivity shows unusual behavior that can be attributed to the structural disorder in this compound. A comparison with the insulating pyrochlore ruthenates underlines the critical role of easily polarizable Pb/Bi ions in inducing the metallic properties and structural modifications observed in these compounds.

DOI: [10.1103/PhysRevB.73.193107](https://doi.org/10.1103/PhysRevB.73.193107)

PACS number(s): 74.70.Pq, 71.27.+a, 75.40.Cx, 72.15.-v

The discovery of superconductivity in  $\text{Sr}_2\text{RuO}_4$  (Ref. 1) has resulted in a resurgence of significant interest in metallic ruthenates with various crystal structures. While  $\text{Sr}_2\text{RuO}_4$  with a highly anisotropic electronic structure was shown to exhibit  $p$ -wave spin-triplet superconductivity,<sup>2</sup> investigations into other ruthenates revealed an extremely rich variety of interesting phenomena; these include metallic ferromagnetism in  $\text{SrRuO}_3$ ,<sup>3</sup> metamagnetism and quantum criticality in  $\text{Sr}_3\text{Ru}_2\text{O}_7$ ,<sup>4</sup> non-Fermi-liquid behavior in  $\text{La}_4\text{Ru}_6\text{O}_{19}$ ,<sup>5</sup> and quasi-one-dimensional behavior in  $\text{BaRu}_6\text{O}_{12}$ .<sup>6</sup> The sensitivity of the strongly correlated electronic state to the crystal structure underlines the important aspect of ruthenates, and it is of significant interest to understand how ruthenates with various lattice geometries acquire a diversity of ground states. In a recent study,<sup>7</sup> we have shown that pyrochlore  $\text{Y}_{2-x}\text{Bi}_x\text{Ru}_2\text{O}_7$  with strong electron correlation and antiferromagnetic geometrical frustration exhibits significant spin fluctuations and electron mass enhancement when the system approaches a metal-insulator transition. This phenomenon bears strong resemblance to the heavy-fermion behavior in  $\text{LiV}_2\text{O}_4$ ,<sup>8</sup> and suggests that detailed understanding of the metallic pyrochlore ruthenates may shed additional light on the remarkable properties of ruthenates in general.

Pyrochlore ruthenates are cubic compounds with the general formula  $A_2\text{Ru}_2\text{O}_{7-\delta}$  [ $A = \text{Pb}, \text{Bi}, \text{Tl}, \text{Y}$ , or lanthanides (Pr-Lu)], which show various electronic properties depending on the  $A$ -site ion. The important structural framework for the electronic properties is the three-dimensional network of corner-sharing  $\text{RuO}_6$  octahedra, which are linked into zigzag chains along the  $\langle 110 \rangle$  direction. The  $\text{RuO}_6$  network has the composition  $(\text{Ru}_2\text{O}_6)_\infty$ , leaving the seventh set of oxygen atoms and the  $A$  ions to occupy the open spaces. For  $\text{Pb}_2\text{Ru}_2\text{O}_{6.5}$ , exactly a half of the seventh oxygen is missing, and the remaining oxygen shows an ordered configuration.<sup>9</sup>  $\text{Pb}_2\text{Ru}_2\text{O}_{6.5}$  and  $\text{Bi}_2\text{Ru}_2\text{O}_7$  show metallic behavior down to the lowest temperature, while  $\text{Tl}_2\text{Ru}_2\text{O}_7$  shows a metal-insulator transition at  $\sim 125$  K.<sup>10</sup> For  $A = \text{Y}$ , or lanthanide, the system is an antiferromagnetic insulator, and the insulating

behavior originates from the Mott-Hubbard gap in the Ru  $t_{2g}$  bands.<sup>11,12</sup> On the other hand, the metallic behavior in  $\text{Pb}_2\text{Ru}_2\text{O}_{6.5}$  and  $\text{Bi}_2\text{Ru}_2\text{O}_7$  is less well understood. While the larger ionic radius of  $\text{Pb}^{2+}$  and  $\text{Bi}^{3+}$  results in better electron transfer through larger Ru-O-Ru bond angles and shorter Ru-O distances,<sup>13,14</sup> there is some evidence that Pb/Bi  $6p$  states hybridize with the Ru  $t_{2g}$  bands to further increase the bandwidth.<sup>15-17</sup> Perhaps related to this, the optical properties of  $\text{Pb}_2\text{Ru}_2\text{O}_{6.5}$  and  $\text{Bi}_2\text{Ru}_2\text{O}_7$  show a number of anomalous and unexplained features in the low-energy regions.<sup>17,18</sup> In this study, we present the resistivity, magnetic susceptibility, and heat-capacity measurements on  $\text{Pb}_2\text{Ru}_2\text{O}_{6.5}$  and  $\text{Bi}_2\text{Ru}_2\text{O}_7$  single crystals to characterize their metallic behavior. The results show that while  $\text{Pb}_2\text{Ru}_2\text{O}_{6.5}$  is a well-defined Fermi liquid with strong electron correlation,  $\text{Bi}_2\text{Ru}_2\text{O}_7$  exhibits unusual features in the lattice heat capacity and resistivity. The results of structural analysis suggest that the inherent lattice disorder in  $\text{Bi}_2\text{Ru}_2\text{O}_7$  is responsible for these unusual behavior.

For this study, single crystals of  $\text{Pb}_2\text{Ru}_2\text{O}_{6.5}$  and  $\text{Bi}_2\text{Ru}_2\text{O}_7$  were grown from the PbO and  $\text{Bi}_2\text{O}_3\text{-V}_2\text{O}_5$  flux, respectively. A previous study<sup>19</sup> has shown that V does not incorporate into the  $\text{Bi}_2\text{Ru}_2\text{O}_7$  crystals in a detectable amount, and our refinements in the growth conditions<sup>20</sup> resulted in crystals with  $\sim 3$  mm on the edge. For a detailed structural investigation, Rietveld refinements using RIETAN-2000 (Ref. 21) were carried out on the powder x-ray diffraction patterns obtained at 300 K with synchrotron radiation of wavelength  $0.45166 \text{ \AA}$ , at the BL02B2 beamline of SPring-8. No extra peaks associated with the impurity phase were observed in both samples down to the  $\sim 0.1\%$  level, and the refinement was carried out for  $3^\circ \leq 2\theta \leq 40^\circ$  in space group  $F\bar{4}3m$  ( $\text{Pb}_2\text{Ru}_2\text{O}_{6.5}$ ) and  $Fd\bar{3}m$  ( $\text{Bi}_2\text{Ru}_2\text{O}_7$ ). The results are shown in Table I. For  $\text{Pb}_2\text{Ru}_2\text{O}_{6.5}$ , no significant deviation from the nominal composition was observed, and the atomic displacement factors  $B$  converged to values that are close to those obtained with neutron diffraction on a polycrystalline sample.<sup>9</sup> For  $\text{Bi}_2\text{Ru}_2\text{O}_7$ , the previous neutron-

TABLE I. Refined structural parameters. Top:  $\text{Pb}_2\text{Ru}_2\text{O}_{6.5}$  in  $F\bar{4}3m$ , with  $a=10.25310(11)$  Å,  $R_{\text{wp}}=4.23$ ,  $R_1=4.18$ , and  $S=1.98$ . Atomic positions are Pb 16e, Ru 16e, O1 24f, O2 24g, and O' 4d. Middle: Model 1 for  $\text{Bi}_2\text{Ru}_2\text{O}_7$  in  $Fd\bar{3}m$ , with  $a=10.29290(14)$  Å,  $R_{\text{wp}}=3.88$ ,  $R_1=4.80$ , and  $S=2.02$ . Atomic positions are Bi 16d, Ru 16c, O 48f, and O' 8b. Refined occupancy for Bi,  $g(\text{Bi})$ , is 0.9722(27). Bottom: Model 3 for  $\text{Bi}_2\text{Ru}_2\text{O}_7$  in  $Fd\bar{3}m$ , with  $a=10.29280(11)$  Å,  $R_{\text{wp}}=3.74$ ,  $R_1=4.51$ , and  $S=1.95$ . Atomic positions are Bi 96h, Ru 16c, O 48f, and O' 32e. Refined  $g(\text{Bi})$  is 0.1629(4).

Atom	$x$	$y$	$z$	$B(\text{Å}^2)$
$\text{Pb}_2\text{Ru}_2\text{O}_{6.5}$				
Pb	0.87654(17)	= $x$	= $x$	0.699(9)
Ru	0.37637(33)	= $x$	= $x$	0.381(14)
O1	0.3090(18)	0	0	0.45(14)
O2	0.4547(15)	$\frac{1}{4}$	$\frac{1}{4}$	0.45(14)
O'	$\frac{3}{4}$	$\frac{3}{4}$	$\frac{3}{4}$	0.45(14)
$\text{Bi}_2\text{Ru}_2\text{O}_7$ (Model 1)				
Bi	$\frac{1}{2}$	$\frac{1}{2}$	$\frac{1}{2}$	1.823(20)
Ru	0	0	0	0.349(25)
O	0.32443(50)	$\frac{1}{8}$	$\frac{1}{8}$	1.87(16)
O'	$\frac{3}{8}$	$\frac{3}{8}$	$\frac{3}{8}$	1.87(16)
$\text{Bi}_2\text{Ru}_2\text{O}_7$ (Model 3)				
Bi	0	0.23693(32)	= $1-y$	0.889(50)
Ru	0	0	0	0.214(26)
O	0.32535(46)	$\frac{1}{8}$	$\frac{1}{8}$	0.85(14)
O'	0.3931(14)	= $x$	= $x$	0.85(14)

diffraction study<sup>22</sup> found anomalously large  $B$  for Bi when the refinement was carried out with Bi and O' (the seventh oxygen) at the usual 16d and 8b site (model 1 in Ref. 22), respectively, and it was proposed that both Bi and O' are disordered into the displaced 96h and 32e sites (model 3 in Ref. 22). Accordingly, we have performed refinements on both models, and model 3 indeed shows a more reasonable  $B$  value for Bi. Moreover, a small deficiency is found on the Bi site, consistent with the previous study.<sup>22</sup> Although the weak scattering factor of oxygen for x-rays precluded the refinement of oxygen occupancy as a free parameter, a small deficiency can be expected on the O' site.<sup>22,23</sup> Overall, the consistencies found between the neutron-diffraction study on a polycrystalline sample<sup>22</sup> and the present synchrotron x-ray diffraction study on crushed single crystals suggest that the disorder and defects are intrinsic to  $\text{Bi}_2\text{Ru}_2\text{O}_7$  and are associated with the easily polarizable Bi ions.<sup>14</sup> Electrical resistivity was measured with a four-probe ac method at 16 Hz. Heat capacity was measured by the relaxation method using a Quantum Design PPMS. Magnetic susceptibility measurements were performed at 10 kOe on collections of single crystals with a superconducting quantum interference device magnetometer. The contribution from the sample holder, which was less than 3% of the total, has been subtracted from the data.

The magnetic susceptibility  $\chi$  of  $\text{Pb}_2\text{Ru}_2\text{O}_{6.5}$  and

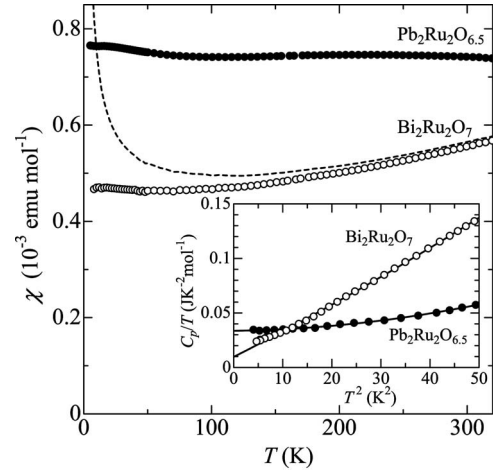


FIG. 1. Magnetic susceptibility of  $\text{Pb}_2\text{Ru}_2\text{O}_{6.5}$  (solid circles) and  $\text{Bi}_2\text{Ru}_2\text{O}_7$  (dashed line) taken under  $H=10$  kOe. A core contribution of  $-1.7 \times 10^{-4}$  emu mol<sup>-1</sup> has been subtracted from the data. For  $\text{Bi}_2\text{Ru}_2\text{O}_7$ , the data accurately follow  $C/T + \chi_0 + \chi_2 T^2$ , and the  $\chi_0 + \chi_2 T^2$  contribution is shown as open circles. Inset: Low-temperature heat capacity of  $\text{Pb}_2\text{Ru}_2\text{O}_{6.5}$  and  $\text{Bi}_2\text{Ru}_2\text{O}_7$ . The lines are the best fits by  $C_p = \gamma T + \beta T^3 + \beta_5 T^5$ . For  $\text{Bi}_2\text{Ru}_2\text{O}_7$ , the fit has been restricted to  $T > 3$  K as described in the text.

$\text{Bi}_2\text{Ru}_2\text{O}_7$  is shown in the main panel of Fig. 1. The data have been corrected for the core diamagnetism of  $-1.7 \times 10^{-4}$  emu mol<sup>-1</sup>. For  $\text{Pb}_2\text{Ru}_2\text{O}_{6.5}$ ,  $\chi$  is almost temperature independent ( $=\chi_0$ ) and shows a relatively large value of  $7.4 \times 10^{-4}$  emu mol<sup>-1</sup> ( $3.7 \times 10^{-4}$  emu Ru mol<sup>-1</sup>), which is characteristic of enhanced Pauli paramagnetism. The Curie contribution observed in previous studies<sup>24</sup> is absent in the present crystals. On the other hand,  $\chi$  for  $\text{Bi}_2\text{Ru}_2\text{O}_7$  (dashed line) decreases gradually with decreasing temperature to a minimum around 100 K, which is followed by a Curie-like increase at lower temperature. For the entire temperature region, the data can be fitted accurately with  $\chi = C/T + \chi_0 + \chi_2 T^2$ , where the first term is a Curie contribution corresponding to 2.5% of  $S=1$  Ru<sup>4+</sup> ions made free by crystal imperfections. The  $\chi_0 + \chi_2 T^2$  contribution is plotted with empty circles in Fig. 1, with  $\chi_0 = 4.6 \times 10^{-4}$  emu mol<sup>-1</sup> ( $2.3 \times 10^{-4}$  emu Ru mol<sup>-1</sup>) and  $\chi_2 = 1.0 \times 10^{-4}$  emu K<sup>-2</sup> mol<sup>-1</sup>. The  $\chi_2 T^2$  contribution originates from the higher-order temperature-dependent term in the Pauli paramagnetic susceptibility, and reflects the shape of the electron density of states at the Fermi energy.<sup>25</sup> The Curie term is slightly larger than that of the polycrystalline sample in the previous study.<sup>7</sup>

For  $\text{Pb}_2\text{Ru}_2\text{O}_{6.5}$  and  $\text{Bi}_2\text{Ru}_2\text{O}_7$ , different contributions to the temperature-independent component  $\chi_0$  must be considered. Since the effective electron mass is enhanced over the free-electron mass, the contribution from the Landau diamagnetism is expected to be small. Although the contribution from the Van Vleck orbital susceptibility is more difficult to assess, NMR studies<sup>26</sup> suggest that it is negligible in these systems. Therefore, the values represented by filled and empty circles in Fig. 1 can be considered to reflect the Pauli paramagnetism in these compounds.

The heat capacity of  $\text{Pb}_2\text{Ru}_2\text{O}_{6.5}$  and  $\text{Bi}_2\text{Ru}_2\text{O}_7$  is plotted as  $C_p/T$  vs  $T^2$  in the inset of Fig. 1. For  $\text{Bi}_2\text{Ru}_2\text{O}_7$ ,  $C_p/T$

displays a small upturn below 3 K, corresponding to the Curie term in  $\chi$ . Accordingly, the data were fitted to  $C_p = \gamma T + \beta T^3 + \beta_5 T^5$  for  $T > 3$  K. Here,  $\gamma T$  is the electronic contribution, and  $\beta T^3 + \beta_5 T^5$  is due to phonons. The same expression was used for  $\text{Pb}_2\text{Ru}_2\text{O}_{6.5}$  down to the lowest temperature, and the results are shown as solid lines in the inset of Fig. 1. For  $\text{Pb}_2\text{Ru}_2\text{O}_{6.5}$ ,  $\gamma = 33.0 \text{ mJ K}^{-2} \text{ mol}^{-1}$  ( $16.5 \text{ mJ K}^{-2} \text{ Ru mol}^{-1}$ ). Together with  $\chi_0$ , we obtain the Wilson ratio  $R_W \equiv (\pi^2 k_B^2 / 3 \mu_B^2) (\chi_0 / \gamma)$  of 1.7 for  $\text{Pb}_2\text{Ru}_2\text{O}_{6.5}$ . This is well within the expected value for strongly correlated systems,<sup>27</sup> implying that both  $\chi_0$  and  $\gamma$  are enhanced by the renormalized electron effective mass, or equivalently, a large density of states at the Fermi level. For  $\text{Bi}_2\text{Ru}_2\text{O}_7$ ,  $\gamma = 10.4 \text{ mJ K}^{-2} \text{ mol}^{-1}$  ( $5.2 \text{ mJ K}^{-2} \text{ Ru mol}^{-1}$ ), which is in good agreement with the value obtained with polycrystalline samples.<sup>7,28</sup> It should be noted that this value is only slightly enhanced over the calculated band value of  $8.0 \text{ mJ K}^{-2} \text{ mol}^{-1}$ ,<sup>15</sup> suggesting only moderate electron correlation and mass enhancement in  $\text{Bi}_2\text{Ru}_2\text{O}_7$ . On the other hand, while the photoelectron spectroscopic measurements<sup>11</sup> also showed a smaller electronic density of states at the Fermi level for  $\text{Bi}_2\text{Ru}_2\text{O}_7$  compared to  $\text{Pb}_2\text{Ru}_2\text{O}_{6.5}$ , the data were analyzed to imply larger electron effective mass in  $\text{Bi}_2\text{Ru}_2\text{O}_7$ . The discrepancy is likely to have arisen in part from the omission of the Bi/Pb  $6p$  contributions in the spectroscopic analysis, which were not recognized at the time. Subsequent band-structure calculations<sup>16</sup> showed that the  $6p$  level is much closer to the Ru  $t_{2g}$  level in  $\text{Bi}_2\text{Ru}_2\text{O}_7$ , resulting in significant hybridization and a broader band. For  $\text{Bi}_2\text{Ru}_2\text{O}_7$ , we obtain  $R_W = 3.2$ , which is slightly larger than  $\text{Pb}_2\text{Ru}_2\text{O}_{6.5}$  but still away from ferromagnetic instability.

The larger slope for  $\text{Bi}_2\text{Ru}_2\text{O}_7$  compared to  $\text{Pb}_2\text{Ru}_2\text{O}_{6.5}$  in the inset of Fig. 1 corresponds to an enhanced phonon contribution in the former compound. Indeed, the  $\beta T^3$  term leads to an unusually small Debye temperature of 210 K for  $\text{Bi}_2\text{Ru}_2\text{O}_7$ , compared to the usual value of  $\sim 550$  K for  $\text{Pb}_2\text{Ru}_2\text{O}_{6.5}$ . As discussed previously,<sup>7</sup> this can be attributed to the lattice softening and localized lattice vibrations arising from the static disorder of Bi- $6s^2$  lone-pair electrons, which correlates with the displacement of Bi ions revealed in the structural analysis. While  $\text{Pb}^{2+}$  ions in  $\text{Pb}_2\text{Ru}_2\text{O}_{6.5}$  also possess  $6s^2$  lone-pair electrons, the displacement in this case is coupled with the oxygen vacancy ordering,<sup>9</sup> and the rigid lattice framework is maintained.

The resistivity  $\rho$  of  $\text{Pb}_2\text{Ru}_2\text{O}_{6.5}$  and  $\text{Bi}_2\text{Ru}_2\text{O}_7$  is shown in Fig. 2. Although both compounds show metallic behavior, there are important differences. For  $\text{Pb}_2\text{Ru}_2\text{O}_{6.5}$ ,  $\rho$  shows a typical behavior of strongly correlated metals, with a small sign of saturation at high temperatures. The lower inset of Fig. 2 shows that  $\rho = \rho_0 + AT^2$  for  $T < 115$  K, indicating the predominant role of electron-electron scattering. The least-squares fit to the data yields  $A = 4.8 \times 10^{-3} \mu\Omega \text{ cm K}^{-2}$ . For  $\text{Bi}_2\text{Ru}_2\text{O}_7$ ,  $\rho$  shows little temperature dependence above  $\sim 170$  K, where it is saturated at  $540 \text{ m}\Omega \text{ cm}$ . Moreover, the previous study<sup>19</sup> on single crystalline  $\text{Bi}_2\text{Ru}_2\text{O}_7$  showed a gradual increase in  $\rho$  at higher temperatures, with a possible plateau feature around the room temperature. Other unusual features in  $\rho$  are also apparent: The residual resistivity is large, with  $\rho(300 \text{ K})/\rho(6 \text{ K})$  of only 1.2, and the low-temperature  $\rho$  follows a  $T^3$  dependence (solid line in the

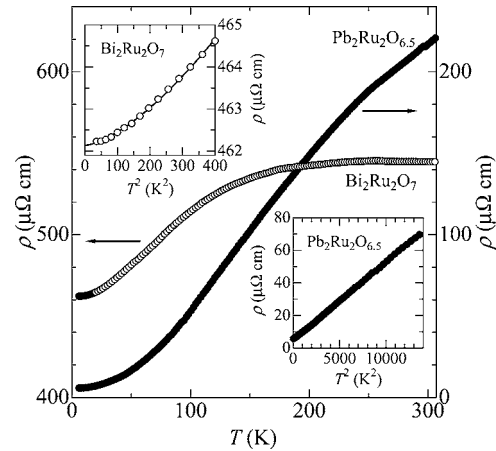


FIG. 2. Electrical resistivity  $\rho$  of  $\text{Pb}_2\text{Ru}_2\text{O}_{6.5}$  (solid circles) and  $\text{Bi}_2\text{Ru}_2\text{O}_7$  (open circles). Insets show the low-temperature data in  $\rho$  vs  $T^2$ . The solid line in the upper inset is a fit to  $\rho_0 + A_3 T^3$ .

upper inset of Fig. 2) rather than a  $T^2$  dependence. While these behaviors are difficult to interpret even qualitatively, a strong scattering of electrons from the disordered lattice and anomalous lattice vibrations is expected to play an important role here.

In Fig. 3, we show the Kadowaki-Woods plot<sup>29</sup> of  $A$  vs  $\gamma$  for  $\text{Pb}_2\text{Ru}_2\text{O}_{6.5}$ , along with a variety of strongly correlated systems.<sup>29–31</sup> The solid line corresponds to the universal value of  $A/\gamma^2 = a_0 \equiv 10 \mu\Omega \text{ cm mol}^2 \text{ K}^2 \text{ J}^{-2}$ , where a number of  $f$ -electron heavy-fermion systems and transition metal oxides (TMOs) appears to follow closely.  $\text{Pb}_2\text{Ru}_2\text{O}_{6.5}$  also follows this trend, demonstrating that same renormalized electrons govern both the enhancement of  $\gamma$  and the electrical transport.<sup>29</sup> Recently, a number of strongly correlated TMOs were shown to possess Kadowaki-Woods ratios that are sig-

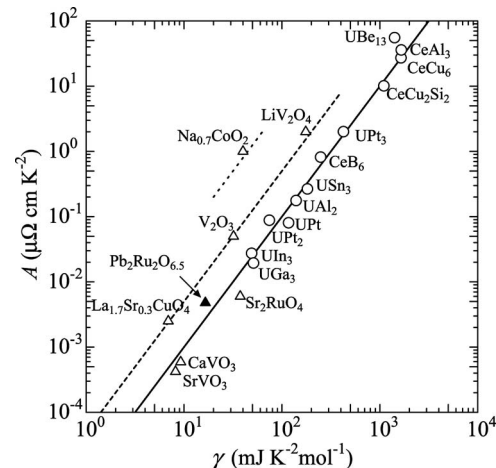


FIG. 3. Kadowaki-Woods plot of the coefficient  $A$  of the  $T^2$  term in the resistivity vs  $\gamma$ , the electronic heat capacity coefficient, for a number of strongly correlated metals (adapted from Refs. 29–31).  $\gamma$  is measured per mole of magnetic ion. The solid line represents the Kadowaki-Woods ratio  $A/\gamma^2 = a_0 \equiv 10 \mu\Omega \text{ cm mol}^2 \text{ K}^2 \text{ J}^{-2}$ , and dashed and dotted lines represent  $5a_0$  and  $50a_0$ , respectively.  $f$ -electron systems are represented by empty circles, whereas  $d$ -electron systems are represented by triangles.

nificantly above the universal ratio. Spinel  $\text{LiV}_2\text{O}_4$ , which has the pyrochlore network of V ions, is a geometrically frustrated heavy-fermion system<sup>8</sup> with  $A/\gamma^2 \sim 5a_0$ . Interestingly, similar values are observed in  $\text{V}_2\text{O}_3$  and  $\text{La}_{1.7}\text{Sr}_{0.3}\text{CuO}_4$ , which are neither geometrically frustrated nor heavy-fermion.  $\text{Na}_{0.7}\text{CoO}_2$  with the triangular geometry of Co ions shows the largest reported value of  $A/\gamma^2 \sim 50a_0$ ,<sup>30</sup> and it was suggested that geometrical frustration may be responsible for the large enhancement of electron-electron scattering.<sup>30</sup> On the other hand, the absence of such an enhancement in  $\text{Pb}_2\text{Ru}_2\text{O}_{6.5}$  suggests that a geometrically frustrated lattice itself is not sufficient to produce the anomalous behavior; in this regard, it is of interest to study  $A/\gamma^2$  when Pb is partially substituted with the rare earth to drive the system closer to an insulator.

To understand the structure and metallic characters of  $\text{Pb}_2\text{Ru}_2\text{O}_{6.5}$  and  $\text{Bi}_2\text{Ru}_2\text{O}_7$ , comparison with the insulating members of  $A_2\text{Ru}_2\text{O}_7$ , where  $A$ =rare earth, is worthwhile. The crystal structures of insulating  $A_2\text{Ru}_2\text{O}_7$  have been studied in detail by both x-ray and neutron-diffraction measurements,<sup>14</sup> and none of the studies so far has shown evidence of disorder at the  $A$  site or significant oxygen deficiency. Accordingly, the structure can be understood as rigid interpenetrating networks of  $\text{Ru}_2\text{O}_6$  and  $A_2\text{O}'$ , and the Mott gap opens at the Fermi level due to the relatively small Ru-O-Ru bond angles ( $\sim 130^\circ$ ) in the pyrochlore. In  $\text{Pb}_2\text{Ru}_2\text{O}_{6.5}$  and  $\text{Bi}_2\text{Ru}_2\text{O}_7$ , the  $6s^2$  lone pair electrons on the Pb/Bi ions result in highly asymmetric bonding with the neighboring  $\text{O}'$  ions, which lead to different consequences for each compound. For  $\text{Pb}_2\text{Ru}_2\text{O}_{6.5}$ , the lone-pair electrons are accommodated by the formation of ordered oxygen vacancy,<sup>9</sup> and the displacement of the Pb ions toward the vacancy can be interpreted as the ordering of the lone pairs in such a direction.<sup>9</sup> On the other hand, oxygen vacancy is much smaller and disordered in  $\text{Bi}_2\text{Ru}_2\text{O}_7$ ,<sup>22</sup> where the small vacancy of Bi also takes place for the charge balance. Accordingly, the highly symmetric  $16d$  site (see Table I) is not com-

patible with the asymmetric Bi ions, and they are randomly disordered into the displaced  $32e$  site.

The difference in the structure exhibited by  $\text{Pb}_2\text{Ru}_2\text{O}_{6.5}$  and  $\text{Bi}_2\text{Ru}_2\text{O}_7$  can be understood to arise from the different stable valence for the Pb and Bi ions. While  $\text{Bi}^{3+}$  is the stable valence in  $\text{Bi}_2\text{Ru}_2\text{O}_7$ ,  $\text{Pb}^{3+}$  is unstable due to the energetically unfavorable configuration of  $6s^1$ . Accordingly, in an ionic picture, either the Pb ions are incorporated into the structure as a 3:1 mixture of  $\text{Pb}^{2+}$  and  $\text{Pb}^{4+}$  with  $\text{Ru}^{4+}$ , or Ru ions as a 1:1 mixture of  $\text{Ru}^{4+}$  and  $\text{Ru}^{5+}$  with  $\text{Pb}^{2+}$ , which are charge balanced with exactly a half of the seventh oxygen missing.<sup>32</sup> Since significant covalent character is expected for Pb-O bonds,<sup>33</sup> the presence of a  $\text{Pb}^{4+}$  state is inconsequential in understanding the average crystallographic structure, which is dictated by the displacement of  $6s^2$  lone-pair electrons. Finally, while the  $6s^2$  lone-pair electrons in  $\text{Pb}_2\text{Ru}_2\text{O}_{6.5}$  and  $\text{Bi}_2\text{Ru}_2\text{O}_7$  influence the structure, they are highly localized and do not participate in the electronic conduction.<sup>15,16</sup> Instead, as discussed above, the metallic behavior is most likely to originate from the extended Pb/Bi  $6p$  band, which can overlap with the Ru  $4d$  band.<sup>15,16</sup> In this regard,  $\text{Pb}_2\text{Ru}_2\text{O}_{6.5}$  and  $\text{Bi}_2\text{Ru}_2\text{O}_7$  are distinct from other metallic ruthenates, where the metallic states arise solely from the Ru-O framework.

In conclusion, we have found that there are significant differences between  $\text{Pb}_2\text{Ru}_2\text{O}_{6.5}$  and  $\text{Bi}_2\text{Ru}_2\text{O}_7$ . While  $\text{Pb}_2\text{Ru}_2\text{O}_{6.5}$  shows the behavior of a well-defined Fermi liquid with strong electron correlation,  $\text{Bi}_2\text{Ru}_2\text{O}_7$  exhibits more unusual behavior that can be explained with the inherent lattice disorder. Since these compounds can be readily tuned to Mott insulators with the  $A$ -site substitution, further investigations should provide an important understanding on the relationship among electron correlation, crystal structure, and exotic behavior in metallic ruthenates.

We thank R. Kanno and Y. Kuroiwa for valuable discussions. The experiment at SPring-8 has been carried out under No. 2005B0620. M.T. has been supported by JSPS.

<sup>1</sup>Y. Maeno *et al.*, Nature (London) **372**, 532 (1994).

<sup>2</sup>A. P. Mackenzie and Y. Maeno, Rev. Mod. Phys. **75**, 657 (2003).

<sup>3</sup>P. B. Allen *et al.*, Phys. Rev. B **53**, 4393 (1996).

<sup>4</sup>S. A. Grigera *et al.*, Science **306**, 1154 (2004).

<sup>5</sup>P. Khalifah *et al.*, Nature (London) **411**, 669 (2001).

<sup>6</sup>Z. Q. Mao *et al.*, Phys. Rev. Lett. **90**, 186601 (2003).

<sup>7</sup>M. Tachibana *et al.*, Phys. Rev. B **71**, 060402(R) (2005).

<sup>8</sup>S. Kondo *et al.*, Phys. Rev. Lett. **78**, 3729 (1997).

<sup>9</sup>R. A. Beyerlein *et al.*, J. Solid State Chem. **51**, 253 (1984).

<sup>10</sup>T. Takeda *et al.*, J. Solid State Chem. **140**, 182 (1998).

<sup>11</sup>P. A. Cox *et al.*, J. Phys. C **16**, 6221 (1983).

<sup>12</sup>J. Park *et al.*, Phys. Rev. B **69**, 165120 (2004).

<sup>13</sup>K.-S. Lee *et al.*, J. Solid State Chem. **131**, 405 (1997).

<sup>14</sup>B. J. Kennedy, Physica B **241-243**, 303 (1998), and references therein.

<sup>15</sup>F. Ishii and T. Oguchi, J. Phys. Soc. Jpn. **69**, 526 (2000).

<sup>16</sup>W. Y. Hsu *et al.*, Appl. Phys. Lett. **52**, 792 (1988).

<sup>17</sup>J. S. Lee *et al.*, Phys. Rev. B **72**, 035124 (2005).

<sup>18</sup>P. Zheng *et al.*, Phys. Rev. B **69**, 193102 (2004).

<sup>19</sup>B. Řehák *et al.*, J. Cryst. Growth **68**, 647 (1984).

<sup>20</sup>A. Harada *et al.* (unpublished).

<sup>21</sup>F. Izumi and T. Ikeda, Mater. Sci. Forum **321-324**, 198 (2000).

<sup>22</sup>M. Avdeev *et al.*, J. Solid State Chem. **169**, 24 (2002).

<sup>23</sup>The refined composition was  $\text{Bi}_{1.90(1)}\text{Ru}_2\text{O}_{6.928(8)}$  in Ref. 22.

<sup>24</sup>T. Akawaza *et al.*, J. Cryst. Growth **271**, 445 (2004).

<sup>25</sup>P. Mohn, *Magnetism in the Solid State: An Introduction* (Springer, Berlin, 2003).

<sup>26</sup>H. Sakai *et al.*, J. Phys. Chem. Solids **63**, 1039 (2002).

<sup>27</sup>M. Imada *et al.*, Rev. Mod. Phys. **70**, 1039 (1998).

<sup>28</sup>S. Yoshii and M. Sato, J. Phys. Soc. Jpn. **68**, 3034 (1999).

<sup>29</sup>K. Kadowaki and S. B. Woods, Solid State Commun. **58**, 507 (1986); K. Miyake *et al.*, *ibid.* **71**, 1149 (1989).

<sup>30</sup>S. Y. Li *et al.*, Phys. Rev. Lett. **93**, 056401 (2004).

<sup>31</sup>I. H. Inoue *et al.*, Phys. Rev. B **58**, 4372 (1998).

<sup>32</sup>Structural studies (Ref. 14) do not rule out either case.

<sup>33</sup>Y. Kuroiwa *et al.*, Phys. Rev. Lett. **87**, 217601 (2001).